# N-Functionalized Poly(dithieno[3,2-*b*:2′,3′-*d*]pyrrole)s: Highly Fluorescent Materials with Reduced Band Gaps

**Katsu Ogawa and Seth C. Rasmussen***

*Department of Chemistry and Molecular Biology, North Dakota State University, Fargo, North Dakota 58105-5516*

*Received November 21, 2005; Revised Manuscript Received January 6, 2006*

ABSTRACT: Oxidative polymerization studies of N-functionalized dithieno[3,2-*b*:2′,3′-*d*]pyrroles (where substituent = hexyl, octyl, decyl, octadecyl, *tert*-butyl, 2-ethylhexyl, or *p*-hexylphenyl) via both chemical oxidation and electropolymerization are presented. While electropolymerized samples are insoluble, it is possible to isolate soluble materials via chemical oxidation methods. Solution and solid-state characterization of the resulting polymeric materials is described, including photophysical and electrochemical studies, and these properties are compared to related polythiophene materials. In addition to reduced band gaps (∼1.7 eV), these materials exhibit good red emission with solution quantum efficiencies up to 34%.

## Introduction

The optical and electronic properties of conjugated organic polymers have led to their use in a variety of applications including batteries, sensors, electrochromic devices, photovoltaics, organic light-emitting diodes (OLEDs), and field effect transistors (FETs).[1] Among these, increasing interest has been devoted to the area of OLEDs.[2] A potential advantage of utilizing conjugated polymers in such applications is the ability to tune the polymer properties at the molecular level, typically accomplished through synthetic modification of monomeric precursors via the incorporation of side-chain functionalities or alteration of the electronic structure of the backbone.[3−5]

The electronic and optical properties of conjugated polymers are largely dependent on the extent of conjugation, which in turn is dependent on the extent of backbone planarity. While many conjugated polymers contain side chains for increased solubility, the inclusion of these side chains typically produce steric interactions that lead to distortions of the backbone planarity. Such deviations from planarity can be due to either interactions between side chains or interactions between the α-units of a side chain and the polymer backbone.[6] Such unwanted steric interactions can be reduced by controlling the side-chain density[6] and the polymer regioregularity[7] or by reducing the size of the α-unit.[8]

Another approach to tuning polymer properties is the annulation of aromatic rings within the repeating units. Such ring fusions introduce rigidity to the backbone, resulting in increased planarity and longer conjugation lengths. The use of various fused-ring precursors has been found to be a powerful approach to the production of low band gap, conjugated polymers.[5,9] However, the synthesis of such precursors can be very laborious, especially if one wishes to incorporate side chains necessary for polymer solubility.

We have previously reported the development of a new general synthetic route to N-functionalized dithieno[3,2-*b*:2′,3′-*d*]pyrroles (DTPs, **1**, Figure 1) which is both simple and efficient.[10] This new synthetic route has allowed convenient access to the desired long-chain alkyl-functionalized precursors needed for the production of soluble polyDTPs, and we recently reported a brief preliminary study of these materials.[8] Here we report the full details of the oxidative polymerization studies of the *N*-alkyl DTPs as well as complete electrochemical and photophysical characterization of the resulting polyDTPs. While Zotti and co-workers have previously reported electropolymerized polyDTPs, the materials produced were insoluble, and characterization of the polyDTPs was limited to the solid state.[11] In addition, these studies were quite limited in the variety of side chains due the difficulties associated with the previous synthetic routes to DTPs. The combination of the new synthetic route to the desired DTP monomers and the development of polymerization conditions for the production of soluble materials have allowed the first full evaluation of these fused-ring polythiophenes as presented in Figure 1.

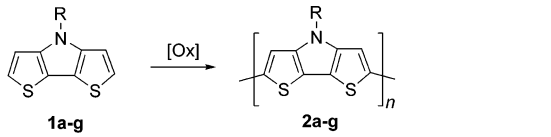


**Figure 1.** Monomeric and polymeric N-functionalized DTPs.

## Experimental Methods

Unless noted, all materials were reagent grade and used without further purification. All glassware was oven-dried, assembled hot, and cooled under a dry nitrogen stream before use. All reactions were performed under nitrogen. $^1$H and $^{13}$C NMR spectra were obtained in $CDCl_3$ on a Varian 300 MHz spectrometer and referenced to the chloroform signal, and peak multiplicity was reported as follows: s = singlet, d = doublet, t = triplet, m = multiplet. High-resolution mass spectrometry was performed in house using a Bruker BioTOF III with an Agilent ES tuning mix as the reference.

**Monomer Synthesis.** N-functionalized DTPs **1a**−**c, 1e**, and **1g** were synthesized as previously reported.[10] Monomers **1d** and **1f** were prepared by analogous procedures. All monomers could be successfully prepared on scales up to 30−40 mmol (∼6−8 g of isolated product) without any decrease in yields compared to the reported procedure.

***N*-Octadecyldithieno[3,2-*b*:2′,3′-*d*]pyrrole (1d):** 61% yield; mp 45.9−46.3 °C. $^1$H NMR ($CDCl_3$) $\delta$: 7.133 (d, $J$ = 5.4 Hz, 2H), 7.009 (d, $J$ = 5.4 Hz, 2H), 4.193 (t, $J$ = 7.2 Hz, 2H), 1.866 (m, 2H), 1.265 (m, 30H), 0.892 (t, $J$ = 6.9 Hz, 3H). $^{13}$C NMR ($CDCl_3$)

* Corresponding author. E-mail: seth.rasmussen@ndsu.edu.

10.1021/ma052490r CCC: $33.50 
Published on Web 02/03/2006

$\delta$: 145.66, 123.49, 115.32, 111.70, 48.17, 32.69, 31.13, 30.47 (3C), 30.43 (3C), 30.41, 30.37, 30.33, 30.22, 30.14, 30.01, 27.75, 23.47, 14.91. HRMS calcd for $C_{26}H_{41}NS_2$: 431.2680; found: 431.2680.

***N*-(2-Ethylhexyl)dithieno[3,2-*b*:2′,3′-*d*]pyrrole (1f):** 48% yield. $^1$H NMR ($CDCl_3$) $\delta$: 7.139 (d, $J = 5.4$ Hz, 2H), 7.001 (d, $J = 5.4$ Hz, 2H), 4.066 (m, 2H), 1.967 (m, 1H), 1.335 (m, 8H), 0.920 (m, 6H). $^{13}$C NMR ($CDCl_3$) $\delta$: 146.05, 123.46, 115.28, 111.87, 52.06, 41.23, 31.39, 29.44, 24.78, 23.77, 14.85, 11.46. HRMS calcd for $C_{16}H_{21}NS_2$: 291.1115; found: 291.1117.

**Chemical Polymerization.** Chemical polymerization was accomplished utilizing modifications of previous literature methods.[6a,12] The desired DTP (1 mmol) was dissolved in dry chloroform (100 mL), followed by the addition of anhydrous $FeCl_3$ (1 mmol). The mixture was allowed to stir under nitrogen for 24 h, poured into methanol (300 mL), and stirred vigorously for 30 min. The resulting precipitate was collected by vacuum filtration, washed with methanol, and air-dried. The polymer was ground into fine powder and purified via Soxhlet extraction with aqueous hydrazine for 24 h, followed by methanol for 24 h. The resulting black powder was dried under vacuum for 2 h.

**Gel Permeation Chromatography.** All GPC experiments were performed on a 500 × 10 mm Jordi Gel DVB 5 $\mu$m mixed-bed column with a Shimadzu SPD-M 10A VP UV absorbance CCD detector at 500 nm. Molecular weights were referenced to polystyrene standards (Aldrich). Polymer samples were prepared in THF (1 mg/mL) and passed through a 0.45 $\mu$m filter prior to injection. A constant flow rate of 1.5 mL/min was used.

**Electrochemistry and Electropolymerizations.** All electrochemical methods were performed on a Bioanalytical Systems BAS 100B/W electrochemical analyzer. Electropolymerizations were carried out in a three-electrode cell consisting of a platinum disk working electrode, a platinum wire auxiliary electrode, and a silver wire quasi-reference electrode. Solutions consisted of monomer (0.01 M) dissolved in spectrochemical grade $CH_3CN$ dried over molecular sieves. The supporting electrolyte was 0.10 M tetrabutylammonium hexafluorophosphate ($TBAPF_6$). The solutions were deoxygenated by sparging with argon prior to each scan and blanketed with argon during the polymerizations. The platinum disk working electrode was polished with 0.05 mm alumina and washed well with deionized water and dry $CH_3CN$ prior to each film growth. The films were grown at a constant potential ~0.1 V positive of the peak potential corresponding to the monomer oxidation. The polymer-coated electrode was then removed, washed with $CH_3CN$, and placed in a cell with a fresh electrolyte solution.

Cyclic voltammetry (CV) weas carried out in the cell described above, substituting a $Ag/Ag^+$ reference electrode (0.251 V vs SCE)[13] for the silver wire quasi-reference. All scans were performed at a sweep rate of 100 mV/s, and solutions were argon sparged and blanketed as described above. Postpolymerization cycling was then performed until a stable, reproducible CV was obtained.

**Solution-Cast Film Formation.** THF solutions of polyDTPs were cast onto glass and slowly evaporated to form a thin film. To better promote uniform film formation, the glass slides were first treated with TMS chloride.[14] The polymers with straight alkyl and aryl side chains (**2a**−**d, 2g**) form uniform thin films, while those with branched alkyl chains (**2e, 2g**) tended to aggregate, resulting in poor films. Similar trends were also observed in film formation on ITO via electropolymerization.

**Absorption and Emission Spectroscopy.** UV−vis spectroscopy was performed on a dual-beam scanning UV−vis−NIR spectrophotometer using samples prepared as dilute THF solutions in quartz cuvettes or as thin films on either glass or indium−tin oxide (ITO) coated glass slides. Spectroscopy solvents were dried over molecular sieves prior to use. Electrochemically polymerized films were grown as described above, substituting an ITO on glass slide for the platinum disk electrode. After polymerization, the polymer-coated electrode was held at a reducing potential to ensure dedoping of the film and then removed, thoroughly washed with $CH_3CN$, and dried. Spectroscopy was conducted on the films with reference to blank slides (ITO or glass, as necessary). Optical band gaps were defined by the onset of the lowest energy transition. The onset was determined by extrapolation of the steepest slope to intersection with the wavelength baseline.

**Table 1. Effect of Oxidant Equivalents on the Amount of Soluble Material Produced during the Polymerization of 1c**

| $FeCl_3$ equivalents | total polymer yield (%) | soluble content[a] (%) | yield of soluble material (%) |
|---|---|---|---|
| 1.0 | 36 | 90 | 32 |
| 1.5 | 86 | 28 | 24 |
| 2.0 | 98 | 20 | 20 |
| 6.0 | 100 | <5 | <5 |

[a] THF-soluble material.

Emission spectroscopy was performed using dilute THF solutions ($<10^{-5}$ M) at room temperature. Prior to each fluorescence measurement, the absorption spectrum was measured to ensure that the maximum absorption of the solution was less than 0.1. Samples were excited at the absorption maximum, and all spectra were obtained by averaging five scans. Quantum yields were determined using secondary methods with 9,10-diphenylanthracene in cyclohexane as the reference.[15] As the polyDTP data were collected in THF, corrections for the difference in the solvent refractive indices were applied using the following values: 1.426 for cyclohexane and 1.407 for THF.

## Results and Discussion

**Oxidative Polymerization.** All DTPs investigated readily undergo oxidative polymerization using either $FeCl_3$ or electrochemical methods. Initial chemical polymerizations were performed according to literature procedures[6a] using 6 mol equiv of $FeCl_3$. Such methods, however, yielded essentially quantitative amounts of insoluble material (>95%, Table 1), potentially indicating that high molecular weight polyDTPs exhibited low solubility. In an attempt to reduce the molecular weights of the polymer products, the quantity of $FeCl_3$ was reduced to a single molar equivalent. While this decreased the amount of polymeric material produced, the resulting materials were soluble in a number of solvents, and only a minor amount (<10%) of insoluble material was isolated when extracted with THF. To further investigate the effect of the number of oxidant equivalents on the overall yield of soluble material, the polymerization of monomer **1c** was performed with various equivalents of $FeCl_3$. As can be seen in Table 1, while 1 equiv of oxidant gives the lowest yield of total polymeric materials, it produces the highest yield of soluble materials. While a variety of side chains were investigated in order to try to modulate the solubility characteristics, the majority of the resulting polymers exhibited results fairly analogous to polymer **2c**. The exceptions were polymers **2a** and **2e** which were found to exhibit lower solubilities and gave lower yields of soluble products.

The electropolymerization of DTPs was first reported by Zotti and co-workers in 1992, with the polymerization of the unfunctionalized parent and four *N*-alkyl analogues (R = methyl, butyl, octyl, hexadecyl).[11] During the investigation of the electrodeposition of **1a**−**g**, electropolymerizations were initially performed following standard literature conditions for functionalized thiophenes.[6a] Unfortunately, these conditions typically resulted in deposition of solid in the bottom of the electrochemical cell rather than the desired film formation on the working electrode. However, reducing the concentration from 0.1 to 0.01 M resulted in the successful formation of polymer films on the surface of the disk electrode. In the case of DTPs containing branched alkyl chains **(2e, 2f)**, it was found that even lower concentrations with longer deposition times were required in order to successfully form good films, as polymer aggregation interfered with formation of uniform films. The use of such low monomer concentrations for electropolymerization was also

**Table 2. Molecular Weight Data of Unfractionated N-Functionalized PolyDTP Samples**[a]

| entry | $M_w$ | $M_n$ | n |
|---|---|---|---|
| **2a** | 1800 | 1400 | 6.8 |
| **2b** | 2300 | 2000 | 7.8 |
| **2c** | 2700 | 2400 | 8.4 |
| **2d** | 4300 | 4200 | 10.0 |
| **2e** | 1200 | 1000 | 4.9 |
| **2f** | 2300 | 2100 | 8.0 |
| **2g** | 2500 | 2300 | 7.3 |

[a] Samples were eluted in THF at a constant flow rate of 1.5 mL/min. Molecular weights were referenced to polystyrene standards.

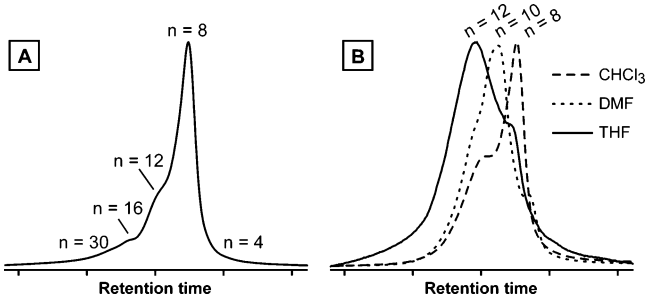


**Figure 2.** GPC chromatogram of **2c** (A) and normalized chromatograms of **2c** solvent fractionations (B).

reported by Zotti and co-workers, who utilized concentrations as low as $2 \times 10^{-3}$ M.[11] All electropolymerized materials were completely insoluble.

**Molecular Weight Analysis.** Molecular weight data for the soluble polyDTP fractions obtained from the $FeCl_3$ polymerizations are summarized in Table 2, and representative GPC chromatograms are shown in Figure 2. It should be noted that the application of polystyrene standards in determining the molecular weights of polythiophenes typically overestimates the size of the polythiophene materials.[16,17] This overestimation is due to the tendency of polythiophenes to adopt a less coiled conformation in solution than polystyrene, and this could be a greater problem in the case of the polyDTPs reported here due to the fused-ring nature of the repeat unit. However, it has also been shown that this overestimation in the case of oligo- and polythiophenes is reduced at lower molecular weights, and thus the small size of the polyDTPs may balance the increased rigidity in any overestimation of molecular weight.

The polydispersity indexes of polyDTPs are relatively narrow (~1.1) and the average number of repeating units increases with the length of side chain. Higher molecular weight samples exhibit limited solubility, and only those samples under 30 repeating units exhibit appreciable solubility in the solvents investigated. The best solvents for solubilizing the polyDTPs were found to be chlorobenzene, THF, chloroform, dichloromethane, and DMF, while slight solubility was seen in diethyl ether, ethyl acetate, acetone, and acetonitrile. The soluble fractions in these latter solvents were found to be smaller oligomers. The polymers were found to be completely insoluble in strongly polar or nonpolar solvents such as hexane, ethanol, methanol, or DMSO.

As can be seen by comparing the results for the straight chain alkyl-functionalized polyDTPs **2a**−**d**, increasing the length of the side chain resulted in the isolation of larger oligomers/polymers. This result can be attributed to some increase in solubility, although the fairly large increase in side chain length from decyl (**2c**) to octadecyl (**2d**) resulted in only a moderate increase in number of DTP units. In attempts to hinder potential aggregation problems that could be limiting solubility, polyDTPs functionalized with branched side chains (**2e,f**) were also

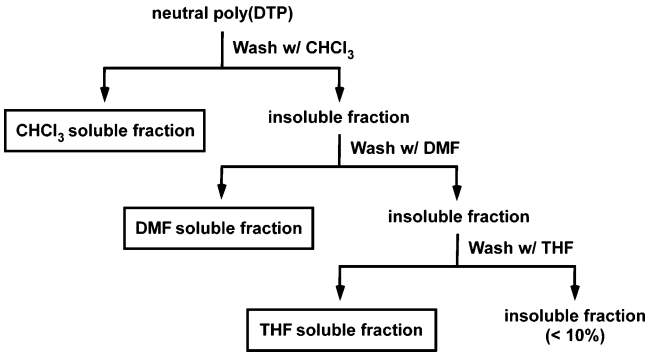


**Figure 3.** Solvent fractionation of polyDTPs.

**Table 3. Molecular Weight Data from the Solvent Fractionation of 2c**[a]

| isolated fraction[b] | $M_w$ | $M_n$ | PDI | *n* | % of total |
|---|---|---|---|---|---|
| no fractionation | 2700 | 2400 | 1.1 | 8.4 | 100 |
| $CHCl_3$-soluble fraction | 2700 | 2400 | 1.1 | 8.4 | 49 |
| DMF-soluble fraction | 3100 | 2800 | 1.1 | 9.6 | 26 |
| THF-soluble fraction | 3600 | 3300 | 1.1 | 11.2 | 25 |

[a] Samples were eluted in THF at a constant flow rate of 1.5 mL/min. Molecular weights were referenced to polystyrene standards. [b] As defined in Figure 3.

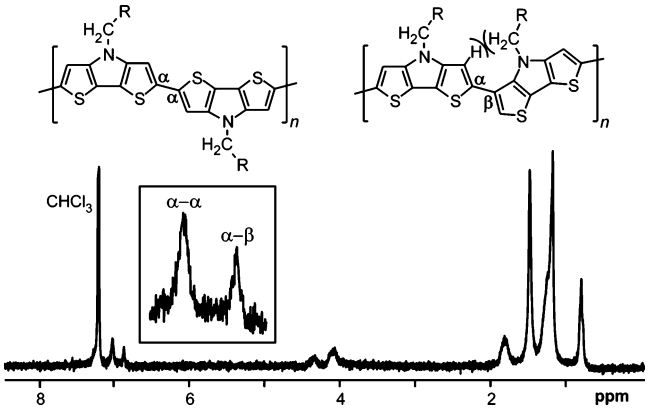


**Figure 4.** NMR spectrum of the $CHCl_3$ solution fraction of **2c**.

investigated. While some slight improvement was exhibited in the case of **2f**, the *tert*-butyl side chains resulted in the least soluble polyDTP, and all isolated samples of **2e** can only be considered oligomeric.

In determining the extent of polymer solubility, it was found that polymer fractions of various molecular weights could be fractionated according to the chosen extraction solvent (Figure 3). Solvents such as $CHCl_3$ solubilize lower molecular weight fractions and thus can be removed by $CHCl_3$ extraction. Chloroform and dichloromethane gave essentially the same results. Further oligomers not soluble in the chlorinated solvents can be removed by DMF, resulting in a final THF-soluble fraction that exhibits higher average molecular weights than the initial unfractionated sample. The results of the various fractionated samples are given in Figure 2 and Table 3.

**Nuclear Magnetic Resonance Spectroscopy.** The $^1H$ NMR spectra of the $CHCl_3$-soluble fraction obtained from the $FeCl_3$ polymerization exhibits two peaks of unequal intensity in the aromatic region corresponding to the DTP ring protons, as shown in Figure 4. The larger of the two peaks agrees well with the position of the monomer $\beta$-proton,[10] while the α-proton cannot be seen above the baseline noise. The absence of a significant peak corresponding to the α-proton end group suggests that the molecular weights determined by GPC are not

**Table 4. Oxidation Potentials of DTPs (1a−g) and PolyDTPs (2a−g)**[a]

| | monomer (**1**) | polymer (**2**) | |
|---|---|---|---|
| entry | $E_{pa}$ (V) | $E_{pa}^{1}$ (V) | $E_{pa}^{2}$ (V) |
| DTP[b] | 0.57 | −0.15 | 0.25 |
| **a** | 0.56 | −0.33 | 0.30 |
| **b** | 0.56 | −0.32 | 0.30 |
| **c** | 0.56 | -0.30 | 0.29 |
| **d** | 0.56 | −0.13 | 0.39 |
| **e** | 0.57 | −0.30 | 0.05 |
| **f** | 0.56 | −0.22 | 0.16 |
| **g** | 0.65 | −0.12 | 0.38 |

[a] Potentials vs $Ag/Ag^+$ measured in millimolar argon-sparged $CH_3CN$ solutions with 0.10 M $TBAPF_6$ as supporting electrolyte. Reported potentials are after cycling to produce a stable, reproducible CV. [b] Unfunctionalized parent: Berlin, A.; Pagani, G.; Zotti, G.; Schiavon, G. *Makromol. Chem.* **1992**, *193*, 399. Adjusted for differences in reference electrode.

grossly overestimated, as oligomers much smaller than those predicted by the GPC measurements should allow us to easily observe the end group α-protons above the baseline noise.

As the smaller of the two peaks does not correspond to either of the original aromatic peaks of the DTP monomers and a defect-free polymer should exhibit only a single aromatic signal, the second peak is attributed to α−β coupling defects within the polymer backbone. This assignment is supported by the additional appearance of two different signals near 4 ppm corresponding to the $C_1$-methylenes of the polymer side chains, which exhibit intensity ratios similar to the two aromatic signals. As shown in Figure 4, α−β defects should maximize interactions between the $C_1$-methylene and the β-position of the neighboring DTP ring. (Modeling of α−β DTP dimers shows this conformation is favored over the inverted conformation due to large steric interactions between the $C_1$-methylene and the neighboring sulfur in the alternate conformation.) The interaction between the aromatic hydrogen and the $C_1$-methylene unit should result in shielding of the aromatic proton, while also deshielding the side-chain methylene, both of which are consistent with the observed minor peaks attributed to the α−β defects.

Coupling defects in the polymer backbone (i.e., α−α vs α−β coupling) are commonly seen in polythiophenes prepared by oxidative polymerization,[4a,7,18] although typically such defects are fairly minor and not to the extent exhibited here. However, during various DTP reactions (brominations, deprotonations, etc.)[19] we have observed that the chemical reactivity difference of the DTP α- and β-positions are significantly less than the ∼95:5 relative reactivity of the parent thiophenes. As such, it is not surprising to witness a greater amount of α−β coupling in the oxidative polymerization of the DTPs. This difference in α vs β reactivity could be attributed to either the influence of the nitrogen adjacent to the β-position, thus increasing its reactivity, or as a result of the ring distortions observed in the crystal structures of DTPs.[10] However, the reactivity of 3-alkylaminothiophenes[8,10] is not consistent with just a simple effect of the nitrogen, and thus the ring distortion may play a significant role. While the NMR spectrum reveals significant α−β defects in the $CHCl_3$-soluble fraction, spectra of the THF soluble fraction in d-THF reveal no obvious defects. It may be that the defects reduce the planarity of the polymer backbone and are thus responsible for the enhanced solubility of the $CHCl_3$ fraction. The high extent of conjugation in the other fractions is also consistent with relatively defect-free samples.

**Electrochemistry.** Cyclic voltammetric (CV) data for the DTPs and their polymers are given in Table 4, and representative cyclic voltammograms of polymer **2c** are shown in Figure 5. CVs of the electropolymerized films generally show a very broad response consisting of multiple oxidative peaks. In most cases, the initial peak is considerably sharper and occurs at potentials below 0 V. This first oxidation is then followed by a stronger broad oxidation that suggests multiple overlapping waves. As seen in Figure 5, potential cycling of the films results in some modification of the CV, most notably in the shifting of the first oxidation peak to lower potential. Zotti and co-workers previously observed similar results in the CVs of poly(octyl-DTP) (**2b**) and attributed this to further polymerization of oligomeric material contained within the polymeric films.[11]

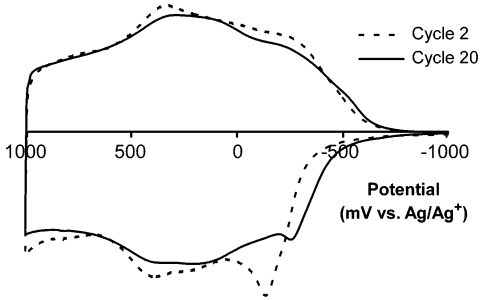


**Figure 5.** Cyclic voltammogram of a polyDTP film 4 **(2c)**.

In comparison to the unfunctionalized parent polyDTP reported by Zotti and co-workers,[11] polyDTPs **2a−g** exhibit similar characteristics although the CVs seem somewhat more broad and less defined. This may be a result of either additional conformational disorder as a result of the side-chain functionalities or slightly thicker films, both of which could result in a greater polydispersity of electroactive sites. Thinner films did exhibit more defined redox waves, but such films were not stable to potential cycling. Repeated cycling of the films resulted in dissolution of some of the film during the negative sweep and production of the neutral film. Comparing the straight-chain alkyl-functionalized polyDTPs **2a−d** reveals little side-chain length dependence, with the exception of polymer **2d**. Here the extremely long octadecyl side chains may introduce additional chain−chain clashes that maximize torsional strain, thus resulting in the shifts of the oxidation waves to higher potential.

Zotti and co-workers noted that overoxidation occurred at potentials greater than 0.7 V.[11] Overoxidation is a common problem among conjugated polymers at higher potentials (∼1.8 V vs $Ag^+/AgCl$) which results in the destruction of the electroactivity of the polymeric material and can compete with electropolymerization.[20] However, as can be seen in Figure 5, potential cycling to 1.0 V results in no oxidative damage to the film. Voltametric study of polyDTPs at higher potential shows that overoxidation begins at ∼1.2 V for **2a−g**. It is possible that the unfunctionalized parent is easier to overoxidize or that the perchlorate electrolyte used in the previous study[11] plays some role in the degradation.

**Absorption Spectroscopy.** As discussed in the molecular weight section above, it is possible to fractionate the polymer samples using sequential solvent extractions. As shown in Figure 6, treatment with various solvents can remove lower MW fractions, resulting in shifts to lower energy in the solution spectra. The GPC data of these isolated fractions indicate an average repeat length of 12 DTP units or less, while the effective conjugation length in polythiophenes has been shown to not reach a limit until ∼20 thiophene rings.[21] Therefore, with the exception of the highest molecular weight fraction, which would correspond to an average of 24 thiophene rings, the other isolated fractions should be comprised of oligomers/polymers below the maximum effective conjugation length. As such, increasing the

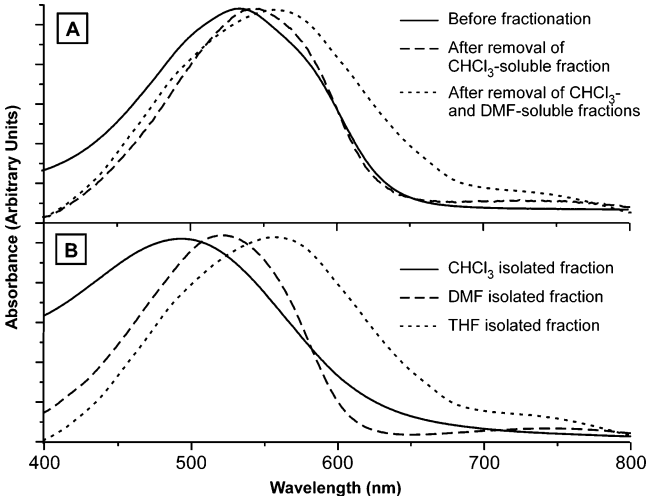


**Figure 6.** Solution (THF) absorption spectra of **2c** after solvent fractionation.

**Table 5. UV−Vis Absorption Data for N-Functionalized PolyDTPs**

| entry | $\lambda_{max}$ (nm,THF)[a] | $\lambda_{max}$ (nm, film)[a,b] | $\lambda_{max}$ (nm, film)[c] | band gap (eV)[d] film | band gap (eV)[d] ITO |
|---|---|---|---|---|---|
| **2a** | 543 | 551 | 545 | 1.68 | 1.71 |
| **2b** | 550 | 555 | 546 | 1.66 | 1.70 |
| **2c** | 552 | 572 | 555 | 1.69 | 1.68 |
| **2d** | 553 | 561 | 600 | 1.68 | 1.64 |
| **2e** | 501 | | 510 | | 1.70 |
| **2f** | 545 | | 547 | | 1.76 |
| **2g** | 514 | 518 | 515 | 1.64 | 1.73 |

[a] $FeCl_3$ polymerized. [b] Solvent cast film on glass. [c] Electropolymerized on ITO. [d] Optical.

average number of repeat units would extend the conjugation length, resulting in the expected red shifts as seen in Figure 6. While DMF washing does increase the average conjugation length of the polymer samples, removal of the residual DMF from the samples is fairly tedious, and thus all samples used for general optical characterization were only fractionated via $CHCl_3$ washing.

Plotting the transition energies of the isolated fractions with the inverse average number of DTP units gives a good linear relationship ($R = 0.99989$) similar to other oligothiophene series.[21,22] Extrapolation to infinite chain length gives an approximate value of 1.25 eV for an ideal polyDTP, which holds significant promise for the production low band gap materials if the low solubility of the polyDTP system can be overcome. A series of discrete oligoDTPs are currently being prepared to allow a more accurate and detailed study on conjugation length dependence in DTP-based materials.

The absorption data for both $FeCl_3$ polymerized and electropolymerized polyDTPs **2a**−**g** are summarized in Table 5. Representative solution and solid-state spectra are shown in Figure 7. In solution, the polyDTPs exhibit broad absorptions with maxima between 530 and 550 nm, with the exception of **2e,** which exhibits a higher energy transition plausibly due to its oligomeric nature and thus shorter conjugation length.

In comparison to regioregular poly(alkylthiophene)s, the polyDTPs exhibit much lower energy transitions in solution, which could be attributed to either the fused-ring nature of the DTPs, the electron-donating influence of the pyrrole nitrogen, or some combination of the two. Typical poly(alkylthiophene)s are thought to adopt a coiled structure in solution with interruptions of conjugation caused by various rotations around the single bonds between thiophene units.[23−26] These rotational

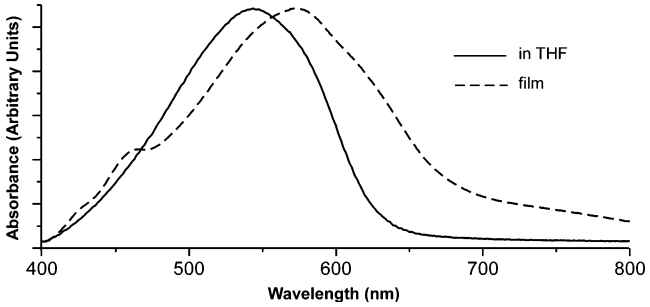


**Figure 7.** Solution- and solid-state absorption spectra of **2c**.

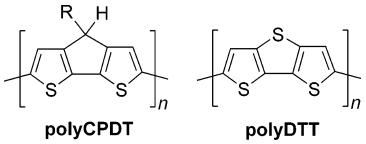


**Figure 8.** Structurally analogous polythiophenes: poly(cyclopenta-[2,1-*b*:3,4-*b*′]dithiophene) (polyCPDT) and poly(dithieno[3,2-*b*:2′,3′-*d*]thiophene) (polyDTT).

defects are thought to be either distributed over just a few monomer repeats or evenly distributed over all monomers.[24,25] In the case of even distribution, theoretical studies have predicted a 34° twist between thiophene units.[27] Because of the fused-ring nature of the DTP units, rotation is not possible within the DTP repeat, and thus half of the possible rotational defects are eliminated. This should result in less coiling in solution and a higher extent of conjugation, thus producing a lower energy transition. However, this does not preclude electronic effects from the central pyrrole ring, and the electronic influence of the pyrrole nitrogen could still have a significant contribution.

To try to understand the relative contribution of both effects, comparison to other analogous fused-ring systems is necessary. The closest structural analogues are the alkyl-substituted poly(cyclopentadithiophene)s and poly(dithieno[3,2-*b*:2′,3′-*d*]thiophene) (Figure 8, polyCPDT and polyDTT, respectively).[28,29] The polyCPDTs contain the structural rigidity of the polyDTPs but lack a conjugated bridgehead and the electron-donating heteroatom. PolyDTT, however, incorporates both rigidity and a central aromatic fused ring, making it the closest known analogue to the polyDTPs. Unfortunately, polyDTT lacks solubilizing side chains, and thus comparisons of solution properties are not possible. We will, however, return to comparisons with polyDTT in the discussion of the solid-state spectra below.

The octyl-functionalized polyCPDT is reported as slightly soluble in $CHCl_3$ and exhibits solution maxima at 560 nm.[28] This transition is actually at slightly lower energy (∼10 nm) than the corresponding polyDTP analogue **2b** and illustrates how large a role simple rigidification can play. This does not preclude contributions from the nitrogen heteroatom but does illustrate that such contributions are not necessary to produce the observed red shifts in the absorption maxima of the polyDTPs. Such comparisons between polyCPDT and polyDTP also agree with previous similarities observed for CPDT- and DTP-based oligomers, which show that changing the bridgehead from CHR to NR results in no change in the absorbance spectra. In fact, for analogous oligomers, the absorbance spectra are superimposable.[19] As a consequence, any electronic contribution from the nitrogen must affect the corresponding HOMO and LUMO equally, thus resulting in no net change in the energy of the HOMO−LUMO transition.

In the transition from solution to solid state, polythiophenes are thought to undergo a coil-to-rod transition producing

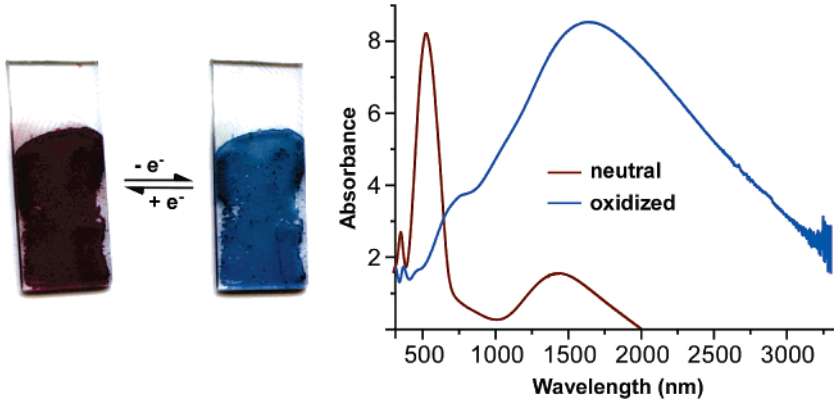


**Figure 9.** Electrochromism exhibited by polyDTP.

extended chains of coplanar thiophene rings. This conformational change coupled with interchain interactions in the solid state results in increased electronic delocalization and a shift of the UV−vis transition to lower energy (Table 5 and Figure 7).[23−26] For the polyDTPs, this shift is somewhat small (∼5−20 nm) in comparison to typical poly(alkylthiophene)s that exhibit bathochromic shifts of up to 90 nm.[6b] This suggests that the shape of the polyDTPs are rather rodlike in solution, unlike most other soluble conjugated polymers. Such a rigid structure could also contribute to the lower solubility exhibited by polyDTPs. Of interest is the fact that the solid-state spectra seem to be somewhat unaffected by the MW distribution of the polymer samples. That is, samples that have not been washed with $CHCl_3$ to remove lower MW oligomers exhibit similar solid-state spectra to those samples that have undergone fractionation, although with larger bathochromic shifts from solution.[8] This may suggest that the $\pi-\pi$ interchain interactions play a major role in the electronic structure of the polyDTP films.

As with the solution spectra, the polyDTP solid-state spectra closely match the alkyl-substituted polyCPDTs (Figure 8). The octyl-functionalized analogue exhibits a solid-state maxima at 590 nm, corresponding to a red shift from solution of 30 nm.[28] As before, this is slightly red-shifted in comparison to the polyDTPs, and the coil-to-rod shift slightly larger, but overall still agrees very well with the polyDTP properties. However, the other structural analogue polyDTT (Figure 8) exhibits its solid-state maxima at ∼460 nm, shifted to the blue by approximately 100−130 nm in comparison to the other two polymer systems.[29] In this case, the bridging sulfur may have a larger electronic effect on the polymer system and could account for this significant difference.[30]

Comparison of the solution-cast and electropolymerized films indicate fairly consistent optical properties, with only a couple cases of significant differences. For the solution-cast films, some chain length dependence is observed. The electrochemically grown films show similar dependence, but to a lesser extent. Increased ordering can sometimes be observed due to side chain packing, which would be enhanced with side-chain length and result in some decrease in the energy of the solid-state absorbance. The lesser dependence in the electrochemically grown films is likely due to the rapid rate of polymer growth, which does not allow for significant self-assembly during deposition. However, the octadecyl-functionalized system does not follow the trend of the series and the electrochemically grown film exhibits significantly better optical properties than the solution-cast film. In the case of the two branched side chains (**2e**, **f**), solution-cast samples only resulted in powdery depositions and sufficient films could not be produced. However, electrochemically grown films could be successfully grown that exhibit transition energies consistent with the other polyDTPs.

As seen in Table 5, all polyDTP samples exhibit moderately reduced band gaps of ∼1.7 eV in comparison of the 2.0 eV band gap of the parent polythiophene. While this value is not as low as the extrapolated value of 1.25 eV discussed above, the properties of the samples may be limited due to their relatively low molecular weights. However, electropolymerized films exhibit similar properties, and thus the band gaps reported here might constitute the limit of the polyDTP system. In comparison to the analogous fused-ring polythiophenes, polyCPDT exhibits band gaps of ∼1.7 eV,[28] while polyDTT exhibits a band gap of 1.9 eV.[29] In all cases, it is evident that ring fusion increases the degree of conjugation and results in a reduction of band gap.

**Electrochromism.** The polyDTP films electropolymerized on ITO exhibit electrochromic behavior undergoing a large switchable color change between the oxidized and neutral states, as shown in Figure 9. As the spectra were not measured in situ, but removed from the electrochemical cell, washed, and then placed in the spectrometer, some minor air oxidation can be seen as evidenced by the peak near 1400 nm in the neutral spectrum. In the oxidized state, the polymer exhibits an intense, broad absorbance with a maximum at ∼1650 nm. The tailing of this transition extends beyond the limit of the instruments capability and would correspond to a band gap of 0.38 eV or less for the oxidized state. Zotti and co-workers previously reported a broad band at 700 nm in the oxidized state of the parent polyDTP.[11] As can be seen in Figure 9, a shoulder is seen at ∼700 nm but is of much lower intensity than the major transition at ∼1650 nm. However, as their study was limited to wavelengths below 900 nm, this lower energy transition would not have been possible to detect. To probe the stability, the potential was varied between −1.0 and 1.0 V for over 30 cycles without any noticeable degradation on the film.

**Emission Spectroscopy**. Solution emission data for the polyDTPs are summarized in Table 6, and a representative emission spectrum is shown in Figure 10. With the exception of polymer **2e**, the polyDTPs exhibit a strong emission around 600−620 nm. The higher energy emission of **2e** is most likely due to its oligomeric nature as discussed above. In comparison to the absorption spectra, the emission is very narrow with typical full width at half-maxima (fwhm) of ∼1200 $cm^{-1}$. This narrowing of the emission band is typical of conjugated polymers and is due to the fact that while the absorption band is due to a wide distribution of conjugation lengths, higher energy absorptions will cascade to lower energy states, and the radiative emission takes place from the lower energy distribution of longer conjugation segments.[29c] However, even in comparison

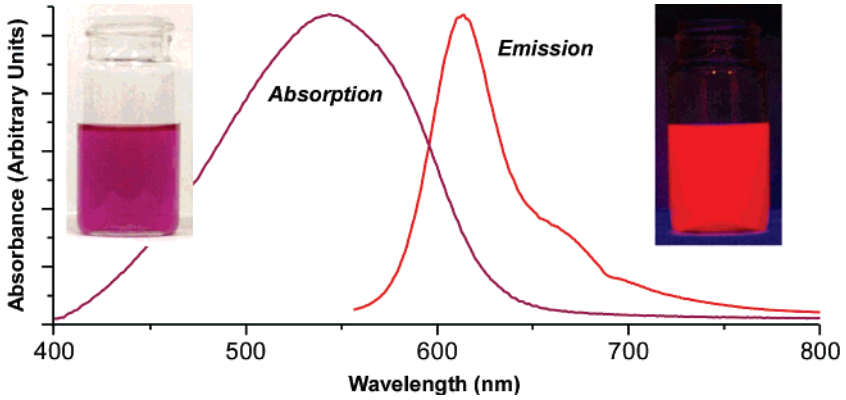


**Figure 10.** Solution absorption and emission spectra of polyDTP (**2c**).

**Table 6. Photophysical Data for N-Functionalized PolyDTPs**[a]

| entry | $\lambda_{ex}$ (nm) | $\lambda_{em}$ (nm) | fwhm$_{em}$ (cm$^{-1}$) | Stokes shift (cm$^{-1}$) | $\Phi_f$ |
|---|---|---|---|---|---|
| **2a** | 543 | 612 | 1271 | 2100 | 0.27 |
| **2b** | 550 | 612 | 1161 | 1800 | 0.31 |
| **2c** | 552 | 614 | 1279 | 1800 | 0.31 |
| **2d** | 553 | 617 | 1076 | 1900 | 0.27 |
| **2e** | 501 | 585 | 2535 | 2900 | 0.30 |
| **2f** | 545 | 604 | 1533 | 1800 | 0.27 |
| **2g** | 514 | 594 | 1971 | 2600 | 0.34 |

[a] $FeCl_3$ polymerized. In THF solution.

to other polythiophenes, the emission bands of the polyDTPs have fwhm that are less than half that of other systems.[31] Such narrowing of the transition is typical of increased rigidity of the polymer backbone in solution,[32] which is consistent with the small bathochromic shifts exhibited in the absorption spectra for the transition from solution to solid state. This backbone rigidity is also supported by the reduced Stokes shift of the polyDTPs (Table 6) in comparison to the typical 5000−6000 cm$^{-1}$ shifts of other polythiophenes.[31−33] As the singlet excited-state of polythiophenes is thought to adopt a quinoid-like structure,[31] a more rodlike ground state would closer match the excited-state geometry, thus resulting in a smaller Stokes shift.[33]

As shown in Figure 10, the polymers have a strong red emission with solution quantum efficiencies of 27−34%. This was initially somewhat unexpected, as monomeric DTPs exhibit significantly less detectable fluorescence ($\Phi_f = \sim 10^{-3}$)[10] than bithiophene ($\Phi_f = 0.026$).[34] The weak fluorescence of thiophene-based chromophores has been attributed to significant spin−orbit coupling thought to be due to the heavy atom effect of the sulfur and is additionally mediated by charge transfer mixing, thus resulting in high triplet quantum yields (0.99 for bithiophene).[34] Highly efficient nonradiative processes between the triplet state and the ground state then leads to relaxation without emission. As the length of the oligothiophene is increased, however, the triplet quantum yields decrease and the fluorescence efficiencies increase.[34] In the case of soluble polythiophenes, the increase in conjugation is offset by the addition of alkyl side chains that lead to additional deactivation pathways via internal conversion.[33] As a result, poly(alkylthiophene)s typically exhibit maximum quantum yields of 26−27%.[31−33] The moderate increase in the polyDTP quantum yields could be the combined result of the reduced number of side chains in comparison to typical poly(alkylthiophene)s, thus reducing coupling modes for internal conversion and the increased rigidity of the polymer backbone.

## Conclusion

N-functionalized polyDTPs were successfully prepared with existing methods to give soluble materials. The resulting polymers can be fractionated by molecular weight due to solubility differences in various solvents, and as a result, defect-rich materials can be removed by simple washes. The low solubilities of the high molecular weight fraction were attributed to the rigid structure of the backbone, as supported by small bathochromic shifts from solution to solid state, small fwhm of emission, and reduced Stokes shifts. The polymers also exhibit enhanced solution fluorescence with quantum efficiencies as high as 34%. All polyDTP samples exhibit moderately reduced band gaps of ∼1.7 eV in their neutral state in comparison of the 2.0 eV band gap of the parent polythiophene, and data suggest that even lower band gaps may be possible in higher MW polyDTPs. The reduced band gaps and increased fluorescence exhibited by these materials suggest that the fused-ring DTP unit is a useful approach to tuning the properties of polythiophenes and holds promise for even further improvements.

**Acknowledgment.** The authors thank the donors of the Petroleum Research Fund, administered by the American Chemical Society, for partial support of this research. Additional support was provided by the ND-EPSCoR "Network in Catalysis" program (NSF-EPS-0132289) and North Dakota State University.

**Supporting Information Available:** IR, $R_f$ data, and $^1$H NMR spectra for compounds **1d** and **1f**; experimental methods and characterization data for synthesis of the precursors to **1d** and **1f**; IR and full GPC data for compounds **2a**−**g**. This material is available free of charge via the Internet at http://pubs.acs.org.

## References and Notes

(1) (a) Schopf, G.; Kossmehl, G. *Adv. Polym. Sci.* **1997**, 129. (b) Katz et al. In *Handbook of Oligo- and Polythiophenes*; Fichou, D., Ed.; Wiley-VCH: Weinheim, 1999; pp 459−490. (c) Kossmehl et al. In *Handbook of Oligo- and Polythiophenes*; Fichou, D., Ed.; Wiley-VCH: Weinheim, 1999; pp 491−524.

(2) (a) Cornil et al. In *Handbook of Oligo- and Polythiophenes*; Fichou, D., Ed.; Wiley-VCH: Weinheim, 1999; pp 317−360. (b) Roman, L. S.; Inganas, O. *Synth. Met.* **2002**, *125*, 419−422. (c) Li, Y.; Vamvounis, G.; Holdcroft, S. *Macromolecules* **2002**, *35*, 6900−6906. (d) Pei, J.; Yu, W. L.; Ni, J.; Lai, Y. H.; Huang, W.; Heeger, A. J. *Macromolecules* **2001**, *34*, 7241−7248. (e) Andersson, M. R.; Thomas, O.; Mammo, W.; Svensson, M.; Theander, M.; Inganas, O. *J. Mater. Chem.* **1999**, *9*, 1933−1940. (f) Yu, G. *Synth. Met.* **1996**, *80*, 143−150.

(3) Baker, G. L. In *Electronic and Photonic Application of Polymers*; Bowden, M. J., Turner, S. R., Eds.; ACS Advances in Chemistry Series 218; American Chemical Society: Washington, DC, 1988.

(4) (a) Roncali, J. *Chem. Rev.* **1992**, *92*, 711. (b) Roncali, J. *Chem. Rev.* **1997**, *97*, 173.
(5) Roncali, J. In *Handbook of Conducting Polymers*, 2nd ed.; Skotheim, T. A., Elsenbaumer, R. L., Reynolds, J. R., Eds.; Marcel Dekker: New York, 1998; pp 311−342.
(6) (a) Rasmussen, S. C.; Pickens, J. C.; Hutchison, J. E. *Chem. Mater.* **1998**, *10*, 1990−1999. (b) Rasmussen, S. C.; Straw, B. D.; Hutchison, J. E. In *Semiconducting Polymers: Applications, Synthesis, and Properties*; Hsieh, B. R., Wei, W., Galvin, M., Eds.; ACS Symposium Series 735; American Chemical Society: Washington, DC, 1999.
(7) McCullough, R. D.; Ewbank, P. C. In *Handbook of Conducting Polymers*, 2nd ed.; Skotheim, T. A., Elsenbaumer, R. L., Reynolds, J. R., Eds.; Marcel Dekker: New York, 1998; pp 225−258.
(8) Ogawa, K.; Stafford, J. A.; Rothstein, S. D.; Tallman, D. E.; Rasmussen, S. C. *Synth. Met.* **2005**, *152*, 137.
(9) Pomerantz, M. In *Handbook of Conducting Polymers*, 2nd ed.; Skotheim, T. A., Elsenbaumer, R. L., Reynolds, J. R., Eds.; Marcel Dekker: New York, 1998; pp 277−309.
(10) Ogawa, K.; Rasmussen, S. C. *J. Org. Chem.* **2003**, *68*, 2921.
(11) Berlin, A.; Pagani, G.; Zotti, G.; Schiavon, G. *Macromol. Chem.* **1992**, *193*, 399.
(12) Sugimoto, R.; Takeda, S.; Gu, H. B.; Yoshino, K. *Chem. Express* **1986**, *1*, 635.
(13) Larson, R. C.; Iwamoto, R. T.; Adams, R. N. *Anal. Chim. Acta* **1961**, *25*, 371.
(14) Umemura, T.; Kasuya, Y.; Odake, T.; Tsunoda, K. *Analyst* **2002**, *127*, 149.
(15) (a) *Standards in Fluorescence Spectrometry*; Miller, J. N., Ed.; Chapman and Hall: New York, 1981; pp 68−78. (b) *Handbook of Organic Photochemistry*; Scaiano, J. C., Ed.; CRC Press: Boca Raton, FL, pp 233−236.
(16) Yamamoto, T.; Oguro, D.; Kubota, K. *Macromolecules* **1996**, *29*, 1833.
(17) Sumi, N.; Nakanishi, H.; Ueno, S.; Takimiya, K.; Aso, Y.; Otsubo, T. *Bull. Chem. Soc. Jpn.* **2001**, *74*, 979.
(18) Leclerc, M.; Diaz, F. M.; Wegner, G. *Macromol. Chem.* **1989**, *190*, 3105.
(19) Radke, K. R.; Ogawa, K.; Rasmussen, S. C. *Org. Lett.* **2005**, *7*, 5253.
(20) Krische, B.; Zagorska, M. *Synth. Met.* **1989**, *28*, C257.
(21) (a) Meier, H.; Stalmach, U.; Kolshorn, H. *Acta Polym.* **1997**, *48*, 379. (b) Izumi, T.; Kobashi, S. Takimiya, K.; Aso, Y.; Otsubo, T. *J. Am. Chem. Soc.* **2003**, *125*, 5286.
(22) Bäuerle, P.; Segelbacher, U.; Maier, A.; Mehring, M. *J. Am. Chem. Soc.* **1993**, *115*, 10217.
(23) Rughooputh, S. D. D. V.; Hotta, S.; Heeger, A. J.; Wudl, F. *J. Polym. Sci., Part B: Polym. Phys.* **1987**, *25*, 1071.
(24) Chen, S.-A.; Ni, J.-M. *Marcomolecules* **1992**, *25*, 6081.
(25) Inganäs, O.; Salaneck, W. R.; Österholm, J. E.; Laakso, J. *Synth. Met.* **1988**, *22*, 395.
(26) Daoust, G.; Leclerc, M. *Macromolecules* **1991**, *24*, 455.
(27) Thémans, B.; Salaneck, W. R.; Bredas, J. L. *Synth. Met.* **1989**, *28*, C359.
(28) Zotti, G.; Schiavon, G.; Berlin, A.; Fontana, G.; Pagani, G. *Macromolecules* **1994**, *27*, 1938.
(29) (a) Jow, T. R.; Jen, K. Y.; Elsenbaumer, R. L.; Shacklette, L. W.; Angelopoulos, M.; Cava, M. P. *Synth. Met.* **1986**, *14*, 53. (b) Taliani, C.; Danieli, R.; Zamboni, R.; Ostoja, P.; Porzio, W. *Synth. Met.* **1987**, *18*, 177. (c) Taliani, C.; Zamboni, R.; Danieli, R.; Ostoja, P.; Porzio, W.; Lazzaroni, R.; Bredas, J. L. *Phys. Scr.* **1989**, *40*, 781.
(30) Zhang, X.; Matzger, A. J. *J. Org. Chem.* **2003**, *68*, 9813.
(31) Belletête, M.; Mazerolle, L.; Desrosiers, N.; Leclerc, M.; Durocher, G. *Macromolecules* **1995**, *28*, 8587.
(32) Theander, M.; Inganäs, O.; Mammo, W.; Olinga, T.; Svensson, M.; Andersson, M. R. *J. Phys. Chem. B* **1999**, *103*, 7771.
(33) Seixas de Melo, J.; Burrows, H. D.; Svensson, M.; Andersson, M. R.; Monkman, A. P. *J. Chem. Phys.* **2003**, *118*, 1550.
(34) Becker, R. S.; de Melo, J. S.; Macanita, A. L.; Elisei, F. *J. Phys. Chem.* **1996**, *100*, 18683.

MA052490R